Preprint of: Mieloszyk E., Abramski M., Milewska A., Determination of the shape of the CFGFT cylindrical column based on laboratory tests, MEASUREMENT, Vol. 232 (2024), 114650, DOI: 10.1016/j.measurement.2024.114650

Determination of the shape of the CFGFT cylindrical column based on laboratory tests

Eligiusz Mieloszyk[a], Marcin Abramski[b], Anita Milewska[c]

Gdansk University of Technology

Abstract

On the basis of laboratory tests of cylindrical composite - concrete columns, analysis of the shape of a buckled column and its coating in the form of a polymer composite pipe reinforced with glass fibers was carried out. Buckling of composite - concrete columns and their coating were analyzed for the angle of the glass fiber beam 20°, 55° and 85°. The studies used non-classical operational calculus and presented various models for determining the shape of the buckled column and its coating. This led to the determination, in the form of modulated harmonic signals, of the shapes of the column and its coating for different models and different angles of the glass fiber beam. The influence of the accuracy of measurements of selected values on the value of critical force was determined and compared for different models.

Keywords: compressive force, composite column coating, shape of the buckled column and its coating

[a] Gdansk University of Technology, ul. Narutowicza 11/12, 80-233 Gdansk, Poland, eligiusz.mieloszyk@pg.edu.pl
[b] Gdansk University of Technology, ul. Narutowicza 11/12, 80-233 Gdansk, Poland, marcin.abramski@pg.edu.pl – corresponding author
[c] Gdansk University of Technology, ul. Narutowicza 11/12, 80-233 Gdansk, Poland, anita.milewska@pg.edu.pl

1. Non-classical operational calculus and the compressed column model

From the point of view of modeling technical systems, the description of phenomena with the use of ordinary or partial differential equations or their sets is of great importance. This concerns the so-called continuous descriptions. A similar situation occurs in discrete descriptions and then the discrete differential equations and their sets are used. There are whole classes of differential equations which, despite a similar shape, describe various technical problems. Differential equations for beams are widely used in practice. Uneven tank settlement causes additional stress in its structure and can lead to its failure, i.e. damage or destruction, which is particularly dangerous in the case of tanks with oil derivatives. Such problems are analyzed using free-standing beam models replacing the tank bottom plate on a rigid base [1], as well as beams taking into account elastic base [2].

Investigation of the influence of small initial cylindrical curvature on deflection of a rectangular plate [3] also comes down to the analysis of a certain differential equation. All these problems, including the problem of an axially compressed articulated rod supported on both sides lead to equations within a certain class of equations.

Due to the wide variety of phenomena described here, it is worth applying a universal form of description using the non-classical operational calculus [4], [5], [6], in which linear operations S, T and s play an important role. Then all the previously mentioned issues, and not only those, can be written in a general form:

$$a_1 Sw + a_0 w = u \ , \tag{1}$$

where u is the input signal, w is the response of the set, while $a_1$and a_0 are coefficients.

As was shown in [5] and [7], type (1) differential problems do not need to have a definite solution. Such a situation is sometimes beneficial, and sometimes not, in contrast to unambiguous solutions that have a specific interpretation. The adoption of an appropriate model of the operational calculus leads to various situations. In the case of beam analysis, it is often enough to use the operational calculus with the S operation specified by the formula:

$$S = \frac{d^2}{dx^2} \tag{2}$$

If in the equation (1) we accept the operation specified by the formula (2) as S, and additionally we assume that $a_1 = 1$, $a_0 = \frac{P}{EI}$, $u = 0$, then we get the equation describing the shape of the neutral axis of the rod / beam / column axially compressed by force P, with EI stiffness, supported on both sides with an articulated joint. This axis is defined as the axis in the cross-section of the column, where longitudinal stresses / strains are not present. For a non-curved beam, not loaded with axial forces, the neutral axis is in the geometric center of the element. The position of the neutral axis is also a function of the state of the structure and is therefore used to create systems for monitoring the technical condition of the structure (Structural Health Monitoring) - [8]. By analogy, we can also create differential models of all the engineering problems mentioned above.

Depending on the method of fixing the beam, appropriate s and T operations should be assigned to the S operation. In the case of a rod / beam / column supported on

both sides with an articulated joint, these operations should be described by the following formulas:

$$Tu(x) = \int_{x_1}^{x}(x-\tau)u(\tau)d\tau + \frac{x-x_1}{x_2-x_1}\int_{x_1}^{x_2}(x_2-\tau)u(\tau)\,d\tau \tag{3}$$

$$sw(x) = w(x_1) + [w(x_2) - w(x_1)]\,\frac{x-x_1}{x_2-x_1} \tag{4}$$

(Operations (3) and (4) are special cases of operations defined in [5].)

Using the formulas (1) - (4) we can create two models of a compressed column.

In model I, we assume that in the entire compression process, both ends of the column with the height h = l do not move. This corresponds to the condition of $sw = 0$, where $x_1 = 0\,, x_2 = l$ - Fig. 1a.

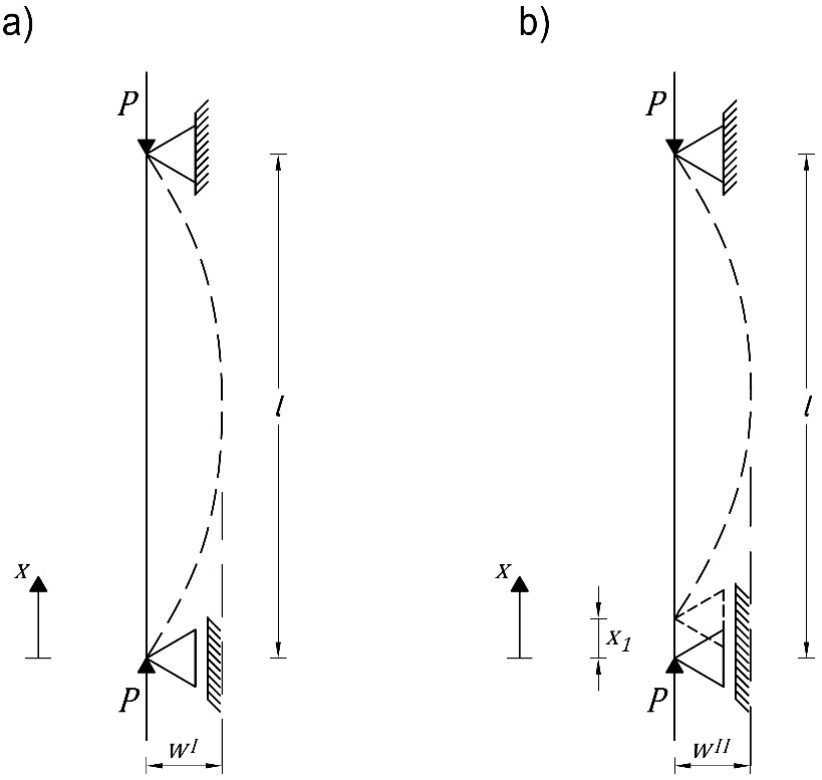

Fig. 1. Axially compressed column: a) model I, b) model II.

In model II, we assume that in the entire compression process one end of the column with height l does not move, and the other moves by a certain amount x_1 - the support is sliding. This corresponds to the condition $sw = 0$, where $x_2 = l$, while x_1 changes - Fig. 1b.

Equation (1) can be represented as a chain connection of generalized first order inertial units [9]. This is particularly important when testing beams / columns with variable cross-section [9]. Using the methods of non-classical operational calculations and defined operations (2), (3) and (4), it is possible to determine buckling y of the column corresponding to the first critical load P_{kr}:

- for model I

$$w^I = Csin\sqrt{\frac{P}{EI}}x = Csin\frac{\pi}{l}x \quad , \tag{5}$$

$$P_{kr}^l = \pi^2\frac{EI}{l^2}$$

– for model II

$$w^{II} = Csin\left[\sqrt{\frac{P}{EI}}(x - x_1)\right] = Csin[\frac{\pi}{l-x_1}(x - x_1)] \quad , \tag{6}$$

$$P_{kr}^{II} = \pi^2\frac{EI}{(l - x_1)^2}$$

where C is a constant.

Constant C in each case can be determined using laboratory experiments for compression of various types of columns, including composite - concrete columns, as we will see later in this paper.

2. Laboratory tests of cylindrical CFGFT type columns [10]

In the laboratory of the Department of Concrete Structures of Gdansk University of Technology, studies were carried out on composite - concrete columns with different heights h=1 and diameters 2r. These were CFGFT (Concrete Filled Glass Fibre – Reinforced Polymer Tube) columns, i.e. poles in the form of a concrete-filled polymer composite tubes reinforced with glass fibers [11]. The composite tube shall be called the coating or column covering. The columns constructed in this way take over the mechanical and strength properties of both materials: those of the composite reinforced with glass fibers and those of the concrete [12]. A batch of CFGFT cylindrical columns with different heights and their coats were tested. In the further part of the paper, we will focus only on columns with a height of h=1=200 cm, for which the column coating is made of a polyester resin tube. The tube was made using a continuous winding method and reinforced with continuous glass fibers [13]. E-type glass fibers used in the production of tubes were in the form of continuous roving with a linear density of 2400 g/m. Tubes with different angles of continuous glass fiber bundles were prepared for the tests - Fig. 2. These were angles 20°, 55° and 85°, and the beam was cross-shaped.

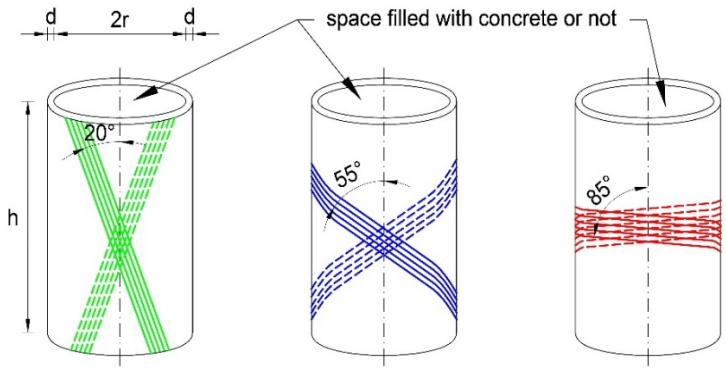

Fig. 2. Scheme of the coating / column cover with the beam angles of the glass fibers marked.

The actual content of glass fibers in the composite was determined by using the standardized method [14], applied in the USA. The test was carried out in the Womach furnace with a maximum heating temperature of 1300°C. According to [14], the furnace was heated up to 535°C during the test. The results obtained from the measurements are presented in Table 1.

The volume content of fibers in the composite given in Table 1 was determined based on the theory of composites [15], according to the formula

$$\bar{f}_v = \frac{\rho_m \bar{f}_g}{\rho_m \bar{f}_g + (100 - \bar{f}_g)\rho_l} \quad , \tag{7}$$

where ρ_m and ρ_l are the densities of the resin matrix and reinforcement fibers, respectively. Their values based on [15] were assumed as 1.1 g / cm^3 and 2.58 g / cm^3 respectively. The other symbols used in formula (7) are defined in Table 1.

Table 1. Fiberglass content in the sample [10]

	For a tube with a beam angle of glass fibers		
	20º	55º	85º
The average proportion of glass fibers in the mass of the sample $\bar{f}_g$[%].	69.3	58.4	72.4
The average square deviation s^2 from the average sample mass [%]^2	2.28	0.59	0.22
s [%]	1.51	0.77	0.47
The average proportion of glass fibers in the sample volume $\bar{f}_v$[%].	49.1	37.5	52.8

It is worth noting that in each case the glass fiber content in the composite declared by the producer was to amount to 60%. As can be seen from Table 1 tests have not confirmed this declaration.

Similar tests were carried out with reference to the inner tube diameter 2r and its thickness d - Fig. 2. Detailed results of these tests can be found in [10]. From these tests it appears that the inner diameter 2r of the tubes was 200 mm, and the thickness d [mm] of their wall was in the range <4.9, 8.8>, with an average wall thickness of 6.5 mm with a standard deviation of about 0.5 mm.

Filling the tested composite pipes with C30/37 grade ready-mix concrete according to Eurocode 2 [16], with a w/c ratio of 0.52, consistency S3 according to standard [17], maximum aggregate grains 16 mm and exposure classes according to standard [18]: XC3, XD2, XF1, XA1 CFGFT columns were prepared. The concrete in the tubes was successively compacted using a depth vibrator from the American company Wacker, model M2000 with a power of 1.5 kW. In addition, tests on the strength of the compressed concrete used were carried out. The average compressive strength received was well correlated with the estimated value of f_{cm}= 38.0 MPa recommended for concrete class C30/37 in standard [16]. All tests were carried out after 80 to 92 days from concreting, which is of particular importance in the case of composite-concrete columns.

Compression of CFGFT columns and their coatings was made using a hydraulic strength press manufactured by the Swiss company Walter + Bai AG, model 102/5000-HK4, with a load capacity of 5000 kN and a press piston extension from 0 to 100 mm.

The load was controlled by the piston stroke of the press. Press tooling enables digital recording of measurement results in the form of discrete signals. Measurement x_1 [mm] of the piston stroke was recorded with an accuracy of 0.01 mm, while the measurement y [kN] of the force values was recorded with an accuracy of 0.1 kN. All tested elements were axially compressed. Support in accordance with previously adopted models was realized as articulated on both sides. Shaft joints (Fig. 3) were used, allowing buckling of columns only in one predetermined plane. The duration of a single experiment was several tens of minutes.

Fig. 3. Composite-concrete column during the test (compression in the press) [10]

On the basis of the research carried out in [19], the functional dependences were determined between the amount of the piston extension and the compressive forces

resulting from this compression. The process mainly used probabilistic methods and metric spaces with various metrics. Selected results are presented in Table 2, limiting only to the beam angles of glass fibers: 20° and 85°, which are representative of the problem under consideration. The symbols in the aforementioned table were adopted as in [19]. (Full analysis and data, including the beam angle of glass fibers 55° can be found in [19].)

Table 2. Selected functional relations between the stroke amount x_1 of the piston and the emerging compressive force y in the case of l = 2000 mm [19]

A	Column coating / covering
A1	The angle of the glass fibers beam 20^0
(A1.1)	$y = 23{,}71x_1\,, \quad x_1 \in < 0{,}10)$
A3	The angle of the glass fibers beam 85^0
(A3.1)	$y = 19{,}89x_1\,, \quad x_1 \in < 0{,}10)$
B	Composite - concrete column
B1	The angle of the glass fibers beam 20^0
(B1.1)	$y = 15{,}63x_1^2 + 81{,}48x_1\,, \quad x_1 \in < 0{,}4)$
(B1.2)	$y = -8{,}81x_1^2 + 318{,}82x_1 - 587{,}30\,, \quad x_1 \in < 4; 9{,}27)$
B3	The angle of the glass fibers beam 85^0
(B3.2)	$y = 10{,}34x_1^2 + 96{,}25x_1\,, \quad x_1 \in < 0{,}6)$
(B3.3)	$y = -10{,}68x_1^2 + 334{,}78x_1 - 686{,}54\,, \quad x_1 \in < 6; 8{,}49)$

The laboratory tests described here will be used to describe the shape of the compressed column and its coating.

3. Determining the shape of a buckled column

As a result of the compression of the column in the hydraulic press, the column buckles. According to model I, its shape is described by the formula (5), while according to model II its shape is described by the formula (6). Model II is closer to the experiment carried out and described earlier. However, model I can also be used to describe the shape of a buckled column, because with small extensions of the piston (especially in the initial compression phase), the sine functions are close to zero. This is therefore some approximation of the II model.

Let us suppose that in the compression process, the phenomenon of shortening of the column is small enough and can be neglected. With this assumption, the following condition must be met: the length of the buckled column must be equal to 1. Using the last condition and the formula for the length of the curve, power series and their properties and the properties of harmonic signals, the following approximate dependences on C appearing in formulas (5) and (6) were received. For: model I:

$$C = \frac{l}{\pi}\sqrt{\frac{2x_1}{l-x_1}} \quad , \quad x_1 \geq 0 \tag{8}$$

Model II:

$$C = \frac{2}{\pi}\sqrt{x_1(l-x_1)} \quad , \quad x_1 \geq 0 \tag{9}$$

Graphs of functions (8) and (9) for l = 2000 mm are shown in Fig.4.

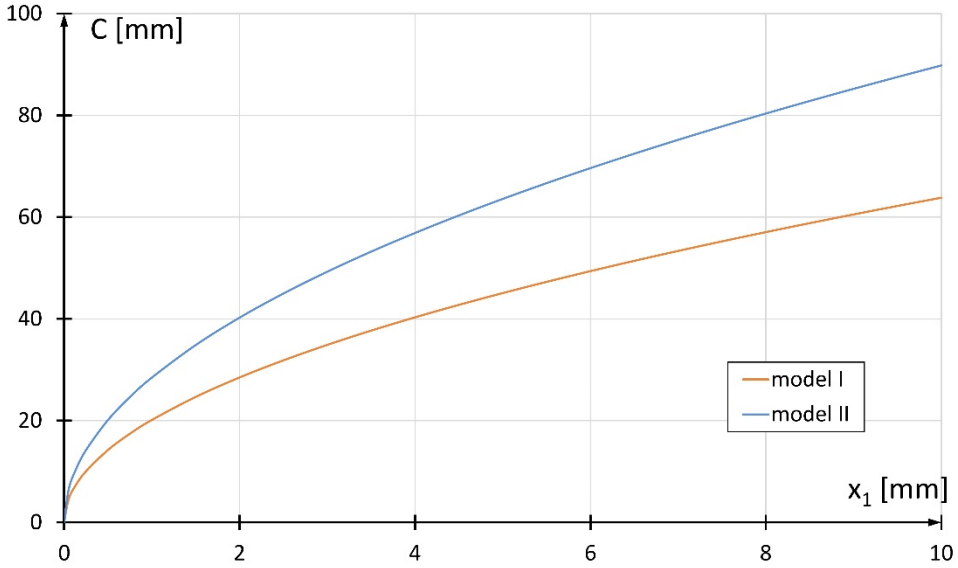

Fig. 4 Graphs C for model I and model II

Conclusion:

From the formulas (8) and (9) it follows that the relationships (5) and (6) show the modulated harmonic signals.

The C function is a non-linear function that grows in both models and is a convex function upwards. The C function values in model I are smaller than the C function values in model II, i.e. the model II closer to the described experiment shows the larger buckling of the column with the same piston stroke sizes.

All functions shown in Table 2 are monotonic functions, more specifically increasing ones. From this it follows that they are reversible, i.e. they have reverse functions. These functions are defined by the formulas shown in Table 3. The following designations were adopted in this table:

$(.)^{-1}$ - corresponding with the designations adopted in [19]. This means the inverse function to the function from the line (.) in Table 2.

Table 3. Selected dependences of the thrust x_1 of the piston as a function of the compressive force y.

A	Column coating / covering
A1	The angle of the glass fibers beam 20^0
$(A1.1)^{-1}$	$x_1 = 0{,}042y \ , \quad y \in < 0; 237 >$
A3	The angle of the glass fibers beam 85^0
$(A3.1)^{-1}$	$x_1 = 0{,}050y \ , \quad y \in < 0; 198{,}9 >$
B	Composite - concrete column
B1	The angle of the glass fibers beam 20^0
$(B1.1)^{-1}$	$x_1 = -2{,}61 + 0{,}06\sqrt{1659{,}75 + 15{,}63y} \ , \quad y \in < 0: 576 >$
$(B1.2)^{-1}$	$x_1 = 18{,}09 - 0{,}11\sqrt{20237{,}44 - 8{,}81y} \ , \quad y \in < 547; 1611 >$
B3	The angle of the glass fibers beam 85^0
$(B3.2)^{-1}$	$x_1 = -4{,}65 + 0{,}05\sqrt{9264{,}063 + 41{,}36y} \ , \quad y \in < 0: 949{,}7 >$
$(B3.3)^{-1}$	$x_1 = 15{,}67 - 0{,}047\sqrt{82748{,}66 - 42{,}72y} \ , \quad y \in < 937{,}7; 1385{,}9 >$

By inserting the dependences contained in Table 3 to the formulas (8) and (9) respectively, we obtain C in the form of a function dependent on the compressive force for model I and model II.

For example, for model II for the coating and the angle of the glass fibers beam 20^0, we have:

$$C = \frac{2}{\pi}\sqrt{0{,}042y\,(l - 0{,}042y)}$$

for $y \in < 0; 237 >$ and l=2000 mm (Fig. 5),

while for the composite-concrete column we will get

$$C = \frac{2}{\pi}\sqrt{-2{,}61 + 0{,}06\sqrt{1659{,}75 + 15{,}63y}\ \left(l + 2{,}61 - 0{,}06\sqrt{1659{,}75 + 15{,}63y}\ \right)}$$

for $y \in < 0: 576 >$ and

$$C = \frac{2}{\pi}\sqrt{15{,}67 - 0{,}05\sqrt{82748{,}66 - 42{,}72y}(l - 15{,}67 - 0{,}05\sqrt{82748{,}66 - 42{,}72y})}$$

for $y \in < 547; 1611 >$ and l=2000 mm (Fig. 7).

Proceeding in the same way, we will get dependences on C for model II. Corresponding graphs for the coating and the column at the fiber glass beam 85^0 are shown in Fig.6 and Fig. 8 respectively.

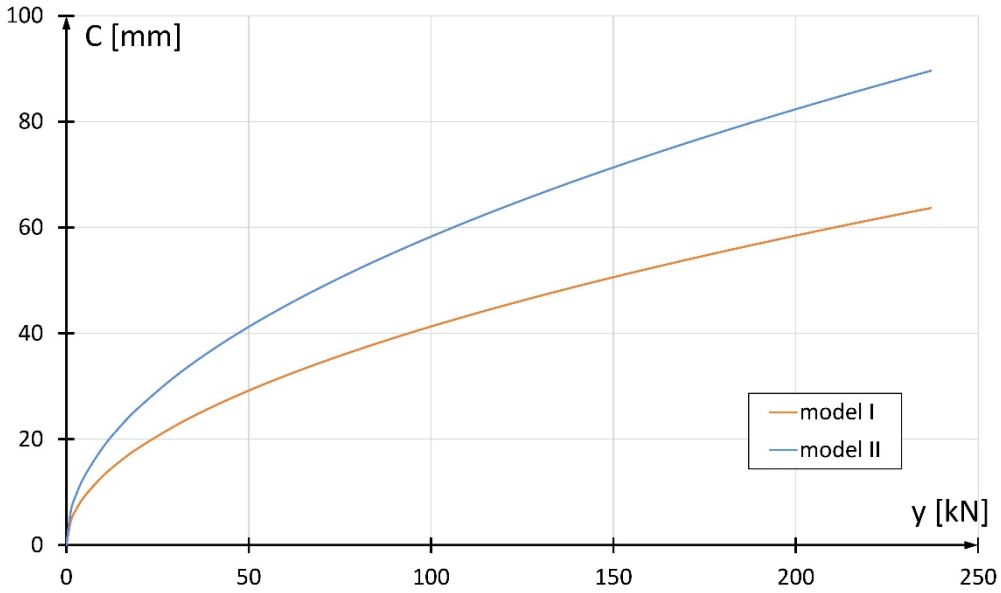

Fig. 5. Graphs C for model I and model II for coating with the fiber glass beam 20^0.

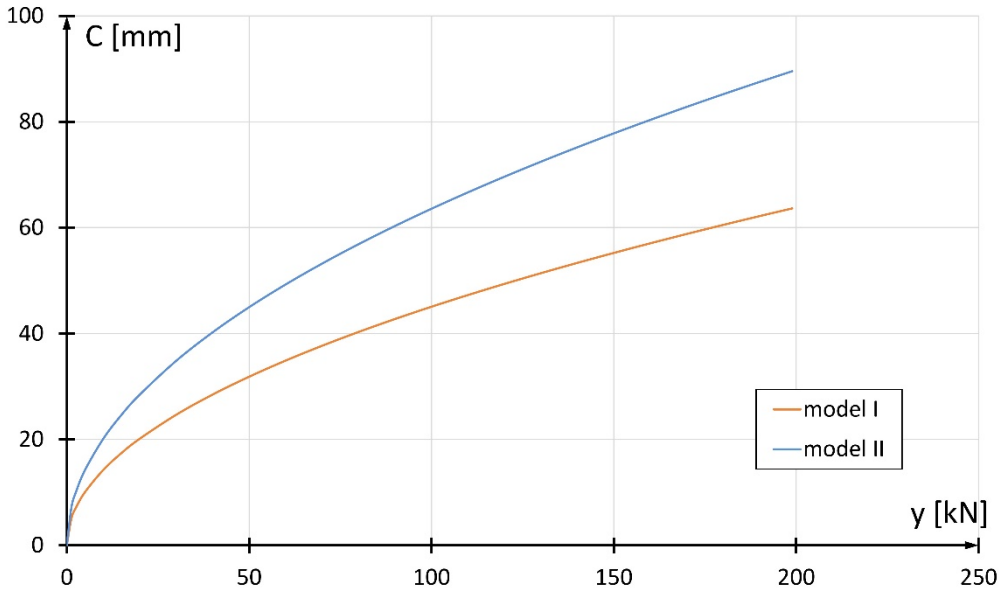

Fig. 6. Graphs C for model I and model II for coating with the fiber glass beam 85^0.

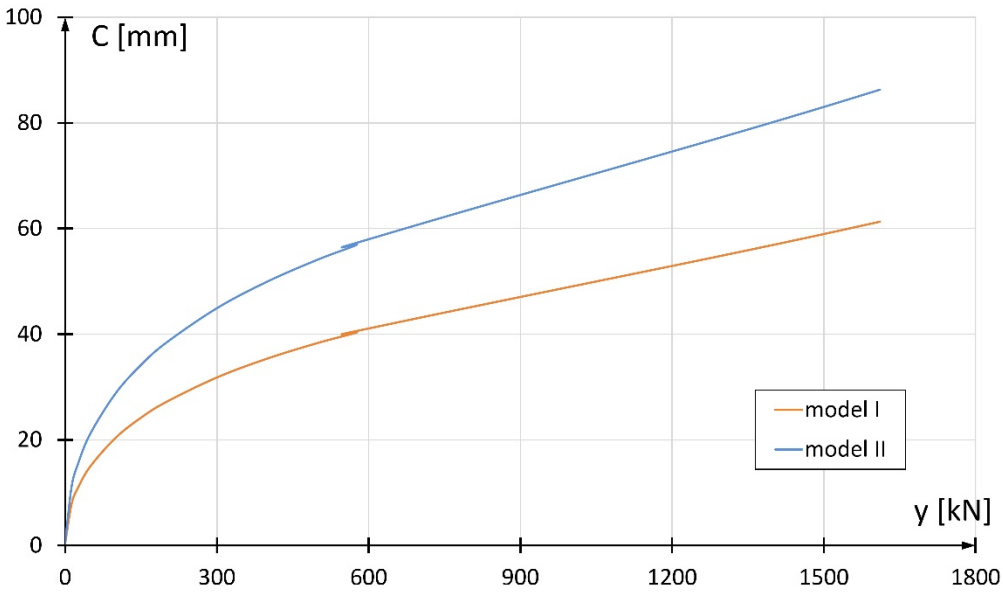

Fig. 7. Graphs C for model I and II in the case of a composite-concrete column with the fiber glass beam 20^0

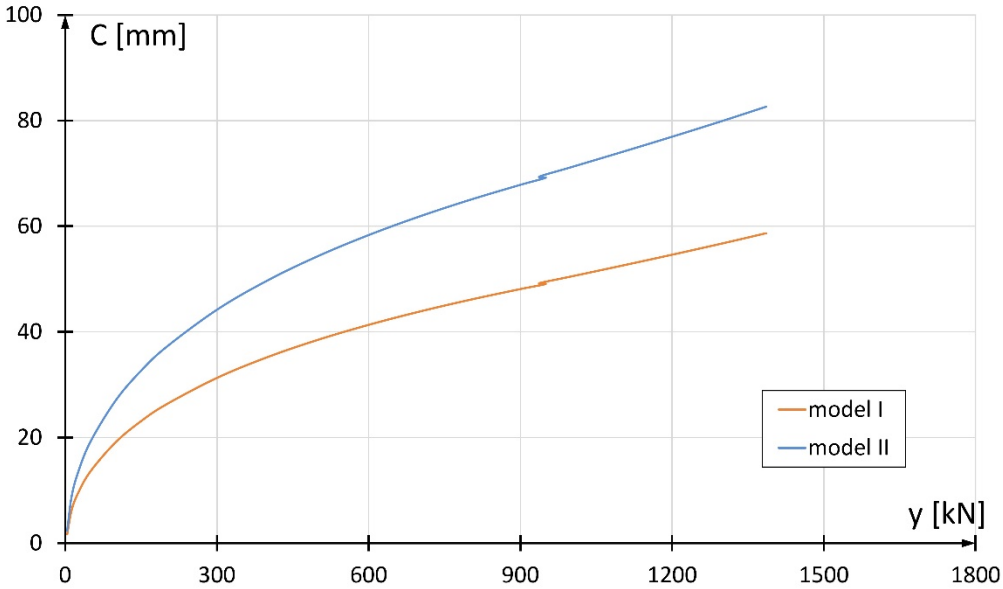

Fig. 8. Graphs C for model I and II in the case of a composite-concrete column with the fiber glass beam 85^0

The graphs show that in each case the C functions have the same character, i.e. they are increasing, convex upwards and bigger for model II than for model I. The values obtained for model II are closer to the real values. This is confirmed only by the analyses of images from experiments, as formal measurements of these quantities during the research were not carried out.

4. Notes on the accuracy of measurements

Let us return to equation (1), and thus to its special case with the S operation described by the formula (2) and leading to the equation of the compressed column. In fact, it is difficult to accurately determine the coefficient $a_0 = \frac{P}{EI}$. Therefore, one should answer the natural question: what effect, for example, on the magnitude of the critical force does an error in determining $a_0 = \frac{P}{EI}$ have?

In [5] it has been shown that if the S operation has the properties required when creating the operational calculus, the new operation $\frac{1}{\alpha}S$, $\alpha > 0$ also has the required properties. Therefore, after using the new operation in the description (1) and after the transformation of the equation (1) the coefficient a_0 will take the form $a_0 = \alpha\frac{P}{EI}$ and then the first critical load for model I determined from it assumes the form:

$$P_{kr}^{\alpha} = \frac{1}{\alpha}\pi^2\frac{EI}{l^2} ,$$

so

$$P_{kr}^{\alpha} = \frac{1}{\alpha}P_{kr}^{I} . \tag{10}$$

From (10) it follows that this correction factor α decides about the influence of the $\frac{P}{EI}$ measurement on the critical force.

Remarks:

If $\frac{P}{EI}$ is underestimated ($\alpha\frac{P}{EI}$, $0 < \alpha < 1$) then P_{kr}^{α} is overestimated.

If the $\frac{P}{EI}$ measurement is overestimated ($\alpha\frac{P}{EI}$, $\alpha > 1$), $then$ P_{kr}^{α} is underestimated.

Analogous reasoning can be carried out for model II and similar conclusions can be formulated.

Additionally, based on formulas (5) and (6), it should be noted that

$$P_{kr}^{II} \geq P_{kr}^{I}.$$

The last formula is of practical importance from the point of view of the design of columns and systems of columns.

5. Conclusions

The traditional construction materials used so far for constructing hybrid columns, such as steel [20], have been successfully replaced by modern composite materials reinforced with glass fibers of various fiber beam angles and subjected to laboratory experimental research.

Experimental research allowed to determine the shape of compressed concrete - composite columns and their coating in the form of modulated harmonic signals.

The use of non-classical operational calculus turned out to be helpful throughout the analysis.

The adopted model has an influence on determining the shape of the buckled column and its coating under the influence of a given compressive force.

The sensitivity of the critical force to changes in the parameters responsible for the technical properties of the column in the differential model describing the behavior of the compressed column has been shown.

Measurement error affects the determination of the magnitude of the critical force.

The use of the proposed models leads to significantly different results.

Generally, the beam angle of glass fibers is not very important in the case of the tests carried out here, however, to precisely determine this impact, we need to consider the curves in metric spaces with an appropriately defined distance shown in Fig.5 - Fig.8.

In the conducted experiments, the shape of columns in the compression process was not recorded.

Coats with a glass fiber beam of 20^0 and 85^0, disregarding the intermediate angle 55^0, were considered, on the basis of [19], to be representative in the research process carried out here.

The proposed model can be helpful in evaluation of structural damages of compressed columns, along with other methods, e.g. wavelet transform [21], [22] or fiber Bragg grating methods.

References

[1] Li G-C. Stress analysis of stepped shell wall and bottom plate of large cylindrical storage. Mechanics and Practice 1979;1:38–41.

[2] Wu TY, Liu GR. Comparison of design methods for a tank-bottom annular plate and concrete ringwall. International Journal of Pressure Vessels and Piping 2000;77:511–7. doi:10.1016/S0308-0161(00)00055-7.

[3] Timoshenko S, Woinowsky-Krieger S. Theory of plates and shells. McGraw-Hill, Inc.; 1959.

[4] Bittner R. Operational calculus in linear spaces. Studia Mathematica 1961;20:1–18. doi:10.4064/sm-20-1-1-18.

[5] Mieloszyk E. Non-classical operational calculus in application to generalized dynamical systems (in Polish). Gdansk: Polish Academy of Sciences Scientific Publishers; 2008.

[6] Mieloszyk E, Grulkowski S. Generalized Taylor formula and shell structures for

the analysis of the interaction between geosythetics and engineering structures of transportation lines. Proceedings of the 11th International Conference Shell Structures. Theory and Application, Gdańsk, Poland: CRC Press Taylor & Francis Group, London; 2017, p. 561–4.

[7] Mieloszyk E. Application of non-classical operational calculus to solving some boundary value problem. Integral Transforms and Special Functions 1998;9:287–92. doi:10.1080/10652460008819262.

[8] Li HCH, Herszberg I, Davis CE, Mouritz AP, Galea SC. Health monitoring of marine composite structural joints using fibre optic sensors. Composite Structures 2006;75:321–7. doi:10.1016/j.compstruct.2006.04.054.

[9] Milewska A. A solution of non-linear differential problem with application to selected geotechnical problems. Archives of Civil Engineering 2011;57:187–97. doi:10.2478/v.10169-011-0014-4.

[10] Abramski M. Short-time load-carrying capacity of columns with a circular cross-section made of FRP tubes filled with concrete. Experiments, theory, calculation. Monograph (in Polish). Gdansk: Gdansk University of Technology; 2019.

[11] Mieloszyk E, Abramski M, Milewska A. CFGFRPT piles with a circular cross-section and their application in offshore structures. Polish Maritime Research 2019;26:128–37. doi:10.2478/pomr-2019-0053.

[12] Ma C-K, Sulaiman MF, Apandi N, Awang AZ, Omar W, Jaw SW. Ductility and stiffness of slender confined reinforced high-strength concrete columns under monotonic axial load. Measurement: Journal of the International Measurement Confederation 2019;146:838–45. doi:10.1016/j.measurement.2019.07.024.

[13] Abdel-Magid B, Lopez-Anido R, Smith G, Trofka S. Flexure creep properties of

E-glass reinforced polymers. Composite Structures 2003;62:247–52. doi:10.1016/j.compstruct.2003.09.022.

[14] ASTM D2584-11: Standard Test Method for Ignition Loss of Cured Reinforced Resins 2011.

[15] Ochelski S. Experimental methods in mechanics of fibre composites (in Polish). Warsaw: Wydawnictwa Naukowo-Techniczne; 2004.

[16] EN 1992-1-1:2004. Eurocode 2: Design of concrete structures - Part 1-1: General rules and rules for buildings 2004.

[17] EN 12350-2: 2009. Testing fresh concrete - Part 2: Slump-test 2009.

[18] EN 206:2013+A1:2016. Concrete – Part 1: Specification, performance, production and conformity. 2016.

[19] Abramski M, Mieloszyk E, Milewska A. Analysis of compressive forces in CFGFT cylindrical pillars and their coatings using laboratory tests and metric spaces. Measurement: Journal of the International Measurement Confederation 2019;142:113–21. doi:10.1016/j.measurement.2019.04.056.

[20] Abramski M. Load-carrying capacity of axially loaded concrete-filled steel tubular columns made of thin tubes. Archives of Civil and Mechanical Engineering 2018;18:902–13. doi:10.1016/j.acme.2018.01.002.

[21] Li H, Yi T, Gu M, Huo L. Evaluation of earthquake-induced structural damages by wavelet transform. Progress in Natural Science 2009;19:461–70. doi:10.1016/j.pnsc.2008.09.002.

[22] Yi TH, Li HN, Sun HM. Multi-stage structural damage diagnosis method based on “energy-damage” theory. Smart Structures and Systems 2013;12:345–61. doi:10.12989/sss.2013.12.3-4.345.